A Novel Method for the Preparation of Lead Selenide: Pulse Sonoelectrochemical Synthesis of Lead Selenide Nanoparticles

Junjie Zhu,† S. T. Aruna, Yuri Koltypin, and A. Gedanken*

Department of Chemistry, Bar-Ilan University, Ramat-Gan 52900, Israel

Received July 21, 1999. Revised Manuscript Received October 18, 1999

PbSe nanoparticles of about 12 nm in size have been prepared by a pulse sonoelectrochemical technique from an aqueous solution of sodium selenosulfate and lead acetate. The PbSe nanoparticles were characterized, using techniques such as transmission electron microscopy, X-ray diffraction, absorption spectroscopy, diffuse reflection spectrum, and energy-dispersive X-ray analysis. The effects of changing the various parameters on particle size were discussed, and possible explanations were offered. A band gap of 1.10 eV was estimated from optical measurement of the nanoparticles.

Introduction

Nanoparticles, nowadays, have become the focus of intensive research due to their numerous applications in diverse fields such as catalyst production, ultramodern electronic and electrooptical devices, supermagnets, photographic suspensions, etc.[1,2]

Semiconductor nanoparticles, in particular, exhibit variable and often controllable properties, especially the change of energy structure and enhanced surface properties with a decrease in size that affects their optoelectronic properties. They have been prepared from many different semiconductors in different forms, such as colloids, powders, and deposits on substrates, and by a variety of methods.[3] One of these methods which has been studied, is electrodeposition to make films of nanocrystals.[4−6]

The interest in lead selenide is due to its narrow band gap, which is employed to produce photoresistors, photodetectors, and photoemitters in the IR range, as well as injection lasers. During the past two decades, PbSe has also been the object of an inquiry into nanosized effects. Lead selenide was synthesized by various methods, including chemical bath deposition,[7] molecular beam epitaxy,[8] vacuum deposition,[9] successive ionic layer adsorption and reaction technique,[10] and electrodeposition.[11,12] Electrodeposition is a simple and low-cost deposition method with many advantages.[13] The deposition process can be controlled more accurately, and the reactions involved are closer to equilibrium than in the many gas-phase methods. Unlike chemical gas-phase methods, electrochemical deposition does not involve the use of toxic gaseous precursors. PbSe has also been prepared by sonicating a mixture of $PbCl_2$ with selenium in ethylenediamine at 18 kHz, using a commercial ultrasonic cleaner. Cubic PbSe nanoparticles were obtained.[14]

Sonochemistry is also a very useful synthetic method which has been in use for some time now. It was discovered as early as 1934 that the application of ultrasonic energy could increase the rate of electrolytic water cleavage.[15] The effects of ultrasonic radiation on chemical reactions are due to the very high temperatures and pressures, which develop in and around the collapsing bubble.[16,17] However, only quite recently has the potential benefit of combining sonochemistry with electrochemistry been increasingly studied. Some of these beneficial effects include acceleration of mass transport, cleaning and degassing of the electrode surface, and an increased reaction rate.[18,19] Marken used a thermostat sonoelectrochemical cell to study homogeneous reactions in solution, and he reported that extremely high limiting currents were detected at significantly negative potentials in the presence of ultrasound.[20] Marken has combined ultrasound and electrochemistry in employing sonoelectrochemical

* Corresponding author. E-mail: gedanken@mail.biu.ac.il. Fax: +972-3-5351250.

† Permanent address: Department of Chemistry, Nanjing University, Nanjing, 210093,China.

(1) Bond, G. C. *Surf. Sci* **1985**, *156*, 966.
(2) Schmidt, G. *Chem. Rev.* **1992**, *92*, 1709.
(3) Fendler, J. H.; Dekany, I. In *Nanoparticle in solid and Solutions*; NATO ASI Series, 3, High Technology; Kluwer Academic Publishers: New York, 1996; Vol. 18.
(4) Golan, Y.; Hodes, G. *J. Phys. Chem.* **1996**, *100*, 2220.
(5) Mastai, Y.; Hodes, G. *J. Phys. Chem. B* **1997**, *101*, 2685.
(6) Lewis, L. N. *Chem. Rev.* **1993**, *93*, 2693.
(7) Gorer, S.; Albu-Yaron, A.; Hodes, G. *Chem. Mater* **1995**, *7*, 1243.
(8) Zogg, H.; Maissen, C.; Masek, J.; Hoshion, T.; Blunier, S.; Tiwari, A. N. *Semicond. Sci. Technol* **1991**, *6*, C36.
(9) Das, V. D.; Bhat, K. S. *J. Mater. Sci* **1990**, *1*, 169.
(10) Kanniainen, T.; Lindroos, S.; Ihanus, J.; Leskela, M. *J. Mater. Chem* **1996**, *6*, 983.
(11) Saloniemi, H.; Kanniainen, T.; Ritala, M.; Leskela, M.; Lappalainen, R. *J. Mater. Chem* **1998**.
(12) Molin, A. N.; Dikusar, A. I. *Thin Solid Film* **1995**, *265*, 3.
(13) Rajeshwar, K. *Adv. Mater* 1992, *4*, 23.
(14) Li, B.; Xie, Y.; Huang, J.; Qian, Y. *Ultrasonics Sonochem.* **1999**, *6*, 217.
(15) Kaplin, A. A.; Bramin, V. A. *Zh. Analit. Khim.* ***1988***, *43*, 921.
(16) Suslick, K. S.; Choe, S. B.; Cichowlas, A. A.; Grinstaff, M. W. *Nature* **1991**, *354*, 414.
(17) Suslick, K. S. *Sci. Am.* **1989**, *260*, 80.
(18) Mason, T. J.; Walton, J. P.; Lorimer, D. J. *Ultrasonics* **1990**, *28*, 333.
(19) Mason, T. J.; Walton, J. P.; Lorimer, D. J. *Ultrasonics* **1990**, *28*, 251.
(20) Marken, F.; Compton, R. *Ultrasonics Sonochem.* **1996**, S131.

10.1021/cm990459w CCC: $19.00
Published on Web 12/17/1999

process.[21−23] They used a high-frequency ultrasound in electrochemical systems for the optimization of electrosynthetic and electroanalytical procedures.[24] Their work has been recently reviewed by Compton and co-workers.[25] Drake found that, during electrodeposition of Cu, 1.2 MHz and 20 kHz ultrasound radiation reduced the diffusion layer from 200 μm to about 20−30 μm and 3.4 μm, respectively.[26] In addition, the electrodeposition of metals or alloys (e.g., Zn, Cu/Zn, Ni/Fe)[27] and the production of catalytically active powders have been reported as a result of combining electrochemistry and ultrasound radiation.

Reisse and co-workers[28−32] have described a novel device for the production of metals, alloys, and semiconductors using pulse sonoelectrochemical reduction. This device exposes only the flat circular area at the end of the sonic tip to the electrodeposition solution. The exposed area acts as both cathode and ultrasound emitter. A pulse of electric current produces a high density of fine metal nuclei. This is immediately followed by a burst of ultrasonic energy, which removes the metal particle from the cathode, cleans the surface, and replenishes the double layer with metal cations by stirring the solution. The metals were obtained as chemically pure, fine crystalline powders of high surface area, with average particle size of 100 nm. Reisse and co-workers[33] reported the first sonoelectrochemical reaction in which a semiconductor, CdTe, was prepared. In their paper, the effect of ultrasound on various electrochemical reactions for the purpose of producing nano-to microparticles of metals and oxides was reported. Grieser and co-workers have also used ultrasonic waves to produce nanoparticles.[34−36] Their work has been recently reviewed by Grieser[37] We have recently described[38] the sonoelectrochemical fabrication of CdSe. The crystal size for CdSe could be varied from X-ray amorphous to 9 nm by controlling the various parameters.

In the present paper, we report the use of the sonoelectrochemical method for the preparation of lead selenide nanoparticles. The sonoelectrochemical device employed by us is similar to that described by Reisse and co-workers.[28−30] Our experiment is based on the electroreduction of selenosulfate in aqueous solution. The as-prepared nanoparticles are ~12 nm in size, as seen using transmission electron microscopy (TEM) and as estimated from the Debye−Scherrer formula.[39] The nanoparticles were also characterized by powder X-ray diffraction (XRD), diffuse reflection spectroscopy (DRS), and energy-dispersive X-ray analysis (EDAX). The optical band gap was also calculated by its DRS spectrum.

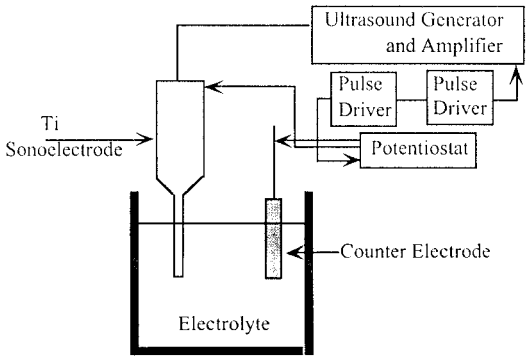

Figure 1. Experimental setup.

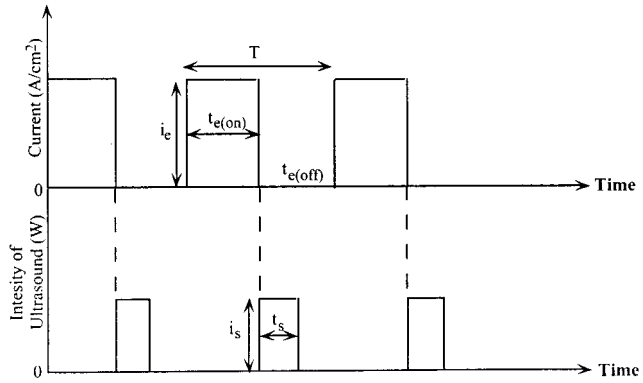

Figure 2. Schematic representation of the sonoelectrochemical wave form.

Experimental Section

The schematics of the experimental setup assembled for these experiments are shown in Figure 1. A titanium horn acted both as the cathode and ultrasound emitter. The electroactive part of the sonoelectrode was the planar circular surface at the bottom of the horn. An isolating plastic jacket covered the immersed cylindrical part. This sonoelectrode produced a sonic pulse that immediately followed a current pulse (Figure 2). One pulse driver (General Valve) was used to control a potentiostat, and a second one (Wavetek function generator 164) to control the ultrasonic processor, which was adapted to work in the pulse mode (Figure 1). PWR-3 power module/potiostat (BAS Inc.) was used to control the constant current regime (without using a reference electrode). A platinum wire spiral (0.5 mm diameter and 15 cm long) was used as a counter electrode. The current pulse was 50mA/cm^2 with a duration of ($t_{e(on)}/t_{e(off)}$) 0.3. The ultrasound pulse intensity was 60W with duration of (t_s) 0.2 s. Because the diameter of sonicator's electrode is 1.13 cm, it so happens that the same

(21) Marken, F.; Rebbitt, T. O.; Compoton, R. G. *Electroanalysis* **1997**, *9*, 19.
(22) Marken, F.; Compton, R. G. *Electrochim. Acta* **1998**, *43*, 2157.
(23) Compton, R. G.; Akkermans, R. P.; Coles, B. A.; Marken, F. *Ultrasonics Sonochem.* **1997**, *4*, 223.
(24) Dei Campo, F. J.; Coles, B. A.; Marken, F.; Compton, R. G.; Cordemans, E. *Ultrasonics Sonochem.* **1999**, *6*, 189.
(25) Compton, R. G.; Eklund, J. C.; Marken, F. *Electroanalysis* **1997**, *9*, 509.
(26) Drake, M. P. *Trans. Inst. Met. Finish* **1980**, *56*, 67.
(27) Mason, T. J. *Chemistry with Untrasound*; Elseriver: London, 1990.
(28) Reisse, J.; Francois, H.; Vandercammen, J.; Fabre, O.; Mesaeker, A. K.-D.; Maerschalk, C.; Delplancke, J. L. *J. Electrochem. Acta* **1994**, *39*, 37.
(29) Chandlerhenderson, R. R.; Coffer, J. L.; Filerreler, L. A. *J. Electrochem. Soc* **1994**, *141*, L166.
(30) Durant, A.; Deplancke, J. L.; Winand, R.; Reisse, J. *Tetrahedron Lett.* **1995**, *36*, 4257.
(31) Dekerckheer, C.; Bartik, K.; Lecomte, J. P.; Reisse. J. *J. Phys. Chem A* **1998**, *102*, 9177.
(32) Durant, A.; Francois, H.; Reisse, J.; KirschDeMesmaeker, A. *Electrochim. Acta* **1996**, *41*, 277.
(33) Reisse, J.; Caulier, T.; Deckerheer, C.; Fabre, O.; Vandercammen, J.; Delplancke, J. L.; Winnand, R. *Ultrasonic Sonochem.* **1996**, *3*, S147−151.
(34) Sostaric, J. Z.; CarusoHobson, R. A.; Mulvaney, P.; Grieser, F. *J. Chem. Soc., Faraday. Trans.* **1997**, *93*, 1791.
(35) Grieser, F.; Hobson, R.; Sostaric, J.; Mulvaney, P. *Ultrasonics* **1996**, *34*, 547.
(36) Sostaric, J. Z.; Mulvaney, P.; Grieser, F. *J. Chem. Soc., Faraday. Trans.* **1995**, *91*, 2843.
(37) Grieser, F. *Stud. Surf. Sci. Catal.* **1997,** *103*, 57.
(38) Mastai, I.; Polsky, R.; Koltypin, Yu.; Gedanken, A.; Hodes, G. *J. Am. Chem. Soc.* **1999**, *121*, 10047.
(39) Klug, H.; Alexander, L. *X-ray Diffraction Procedures*; New York, 1962; p 125.

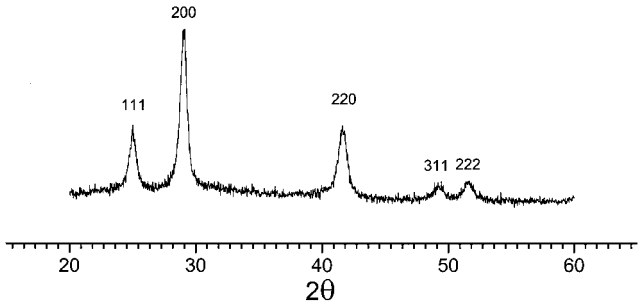

Figure 3. X-ray diffraction pattern of as-prepared PbSe nanoparticles.

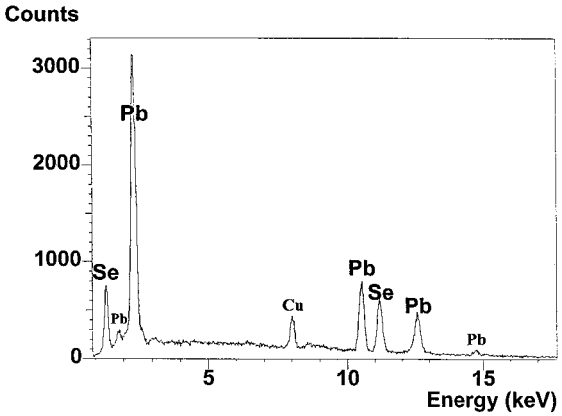

Figure 4. The EDAX pattern of as-prepared PbSe.

numerical values apply to current and to the current density and the value of power intensity is also equal to that of power density.

The electrolyte was based on that used by Hodes and coworker.[40] An aqueous solution of $Pb(Ac)_2$ complexes with sodium nitrilotriacetate ($N(CH_2COONa)_3$−NTA was mixed with an aqueous sodium selenosulfate (Na_2SeSO_3) to give a final concentration of 0.02 M $Pb(Ac)_2$, 0.02 M (Na_2SeSO_3), and 0.04 M NTA at pH 11. The exact composition of the electrolyte is not critical, but it is important that the solution pH be greater than 7 before the addition of Na_2SeSO_3 to prevent the formation of free Se. The electrolyte volume was 50 mL. The deposition was carried out, typically, for 30 min. At the end of the reaction, the precipitate was centrifuged, repeatedly washed with distilled water and acetone, and dried under vacuum.

The instruments used for the characterization in this report for XRD, TEM, EDAX, and DRS measurements have been described elsewhere.[41]

Results and Discussion

XRD, EDAX, and TEM studies. The XRD pattern (Figure 3) of the as-prepared PbSe showed the presence of the diffraction peaks corresponding to the (111), (200), (220), (311), and (222) planes of cubic PbSe. The detected broader peaks indicate that the crystal size is small. The size of the PbSe nanoparticles estimated from the Debye−Scherrer formula is about 12 nm.

The EDAX pattern of the PbSe (Figure 4) showed the presence of Pb and Se peaks. The average atomic ratio of Pb:Se was 57:43, which showed that the samples were rich in lead.

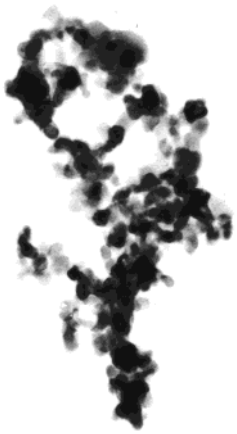

Figure 5. Transmission electron micrograph of the as-prepared PbSe nanoparticles.

The TEM observations for the as-prepared PbSe nanoparticles are shown in Figure 5. It is apparent that PbSe nanoparticles are spherical and that the particles are held together by a porous irregular network. The average size of these nanoparticles is in the range of 10−15 nm, which is in good agreement with the XRD result.

Optical Properties. We have carried out the optical diffuse reflection spectra measurement of PbSe powder in order to resolve the excitonic or interband (valence−conduction band) transitions of PbSe, which allows us to calculate the band gap. Figure 6a depicts the optical diffuse reflection spectrum of the PbSe powder. An estimate of the optical band gap is obtained using the following equation for a semiconductor:

$$\alpha(\nu) = A(h'\nu/2 - Eg)^{m/2}$$

where $h' = h/2\pi$, α is the absorption coefficient, and m is equal to 1 for a direct allowed transition. Since α is proportional to $F(R)$, the Kubelka−Munk function, the energy intercept of a plot of $(F(R)*h\nu)^2$ versus $h\nu$ yields Eg for a direct allowed transition (Figure 6b).[42] From the spectra, we calculated the band gap of PbSe to be 1.10 eV. The value of the band gap energy is larger than that of the reported value for bulk PbSe (0.29 eV).[43] The increase of band gap is indicative of size quantization.[44] For a crystallite size less than the Bohr diameter (~80 nm for PbSe), an increase in the effective band gap due to size quantization should begin to be apparent. Nedeljkovic et al. demonstrated the blue shift in the optical spectra of PbSe.[45] Hodes also reported the quantum effects of lead selenide film. PbSe of different sizes have different band gaps, which vary from 0.55 to 1.55 eV.[40]

Discussion

There are a few experimental variables involved in the sonoelectrochemical deposition: the electrolyte composition and temperature; electrodeposition conditions

(40) Gorer, S.; Albu-Yaron, A.; Hode, G. *J. Phys. Chem.* **1995**, *99*, 16442.
(41) Dhas, N. A.; Zaban, A.; Gedanken, A. *Chem. Mater.* **1999**, *11*, 806.
(42) Luca, V.; Djajanti, S.; Howe, R. F. *J. Phys. Chem. B* **1998**, *102*, 10650.
(43) Streltov, E. A.; Osipovich, N. P.; Ivashkevich, L. S.; Lyakhov, A. S.; Sviridov, V. V. *Electrochim. Acta* **1998**, *43*, 869.
(44) Yang, J. P.; Meldrum, F. C.; Fendler, J. H. *J. Phys. Chem.* **1995**, *99*, 5500.
(45) Nedeljkovic, J. M.; Nenadovic, M. J.; Micic, O. I.; Nozik, A. J. *J. Phys. Chem.* **1986**, *90*, 12.

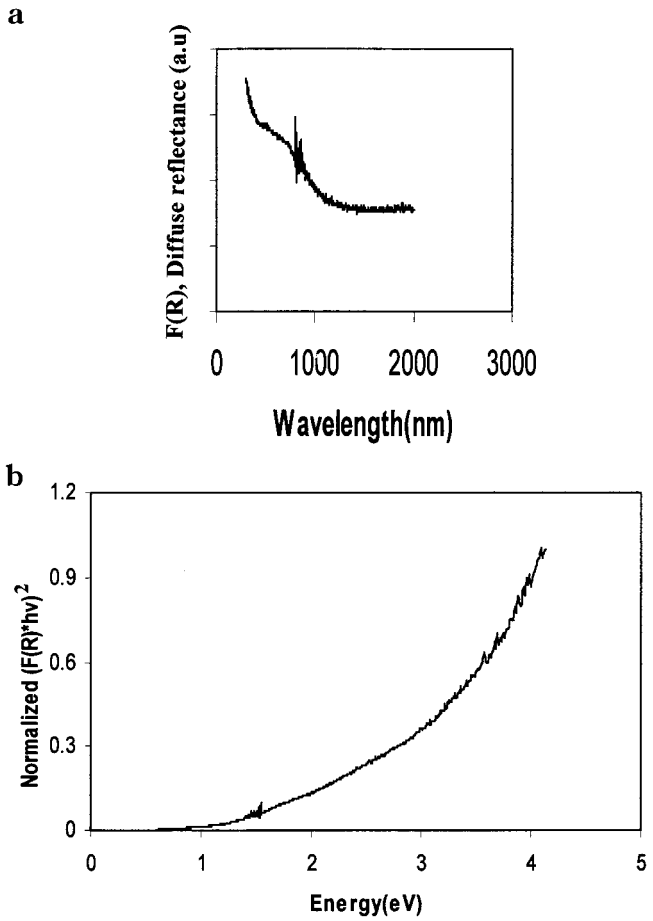

Figure 6. (a) Diffuse reflection spectrum of a glass coated with PbSe nanoparticles, and (b) normalized $(F(R)*h\nu)^2$ versus $h\nu$ (eV) of PbSe nanoparticles.

including current density, pulse on time and ratios between pulse on time and off time (duty cycle); and sonic probe conditions (power, pulse parameters). While we did not carry out exhaustive investigations of the effects of all of these parameters and their effects on the properties of deposited PbSe, we did, however, study a range of deposition conditions. The basis for using a sonoeletrochemical technique to form nanoparticles is the massive nucleation using relatively higher current density electrodeposition pulse (20−120 mA/cm^2 in this work), followed by the removal of the deposit from the electrode by the sonic pulse. Removal of the PbSe from the electrode before the next current pulse prevents crystal growth. The effects of the various parameters on the crystal size were studied, and a rationalization of these results is offered.

We have varied the reaction temperature and measured the dependence of the particle size on temperature. The particle sizes obtained for reactions carried out at 10, 30, and 60 °C were 10, 12, and 13 nm, respectively. Similar results were obtained for the sonoelectrochemical preparation of CdSe. A detailed explanation has been offered for the latter case.[38] We will repeat the main points herein. The temperature can affect crystal growth in several ways, all of them resulting in smaller crystal size at lower temperatures. The simplest explanation is that crystal growth is slower at lower temperatures. Within the time between sonic pulses, growth can occur, either by coalescence during the deposition pulse or by migration on the substrate and coalescence at any time. Also, if the sonic pulse does not completely remove the deposit, there is even more of an opportunity for the crystals on the substance to grow. In addition, the crystals, particularly the smaller ones, might also grow to some extent by coalescence in the electrolyte after removal from the electrode. Another effect of temperature is the thermodynamic instability of small nuclei below a certain critical size. These nuclei should redissolve, but may be stable for a long enough period of time to grow larger than the critical size, after which they are thermodynamically stable. This kinetic stabilization is more effective at lower temperatures; this is a common mechanism to explain the decrease in size that accompanies a decease in temperature. It may also be operative here, although the presence of the heterogeneous substrate (the electrode) can also exert an additional stabilizing influence on nuclei, which would be subcritical in the absence of this surface. Different experimental temperatures were employed.

Sonic intensity also affected the particle size. As implied above, the greater the sonic intensity, the greater will be the efficiency of removal of deposition and therefore the less chance for the crystal growth of existing nuclei. Above a certain intensity wherein all of the deposit is removed, a further increase in intensity is not expected to affect further growth. It is important to note that in the absence of sonic excitation, the PbSe forms as a film on the electrode. When we use 0, 10, and 60 W/cm^2 to carry out experiments, the particle size estimated from the Debye−Scherrer formula is 16, 13, and 12 nm, respectively.

Different deposition current pulse widths influence the size of PbSe. The particle size obtained was 10, 12, and 16 nm for $t_{e(on)}$ 0.1, 0.3, and 1.0 s, respectively. In these three experiments, the same $t_{e(off)}$ of 1 s was employed. Quite separately from the sonic wave effects, pulse electrodeposition is well-known to result in a smaller crystal-sized deposit. This is particularly pronounced for higher current deposits, where a higher rate of nucleating occurs during each pulse. For a shorter pulse duration, the chance for crystal growth to occur by deposition of new material on a previous nucleus is smaller. In normal pulse plating, crystal size may or may not increase with the number of pulses, depending on whether each new pulse forms a new nucleus or adds to preexisting ones. In sonoelectrochemical deposition, where the deposition is removed during each sonic pulse, only new nuclei should be formed, and there the crystal size will be small.

The effect of current density was also taken into account. When current was not employed, and only the sonochemical pulse was applied, no reaction took place. With the increase of current, the size was changed only slightly (14 nm at 20mA/cm^2, 12 nm at 50mA/cm^2, and 10 nm at 120mA/cm^2), but if current was too large, above 120 mA/cm^2, small impurity peaks were detected in the XRD. Current density can affect crystal size in at least two opposing directions. A smaller size would be expected, on the basis of the smaller amount of material deposited at a lower current. On the other hand, lower currents (per unit time) allow more time for atomic diffusion processes to occur which can lead to larger crystal size. In the absence of other effects, it

seems that the latter is dominant in this case. We found that the best conditions for the fabrication of PbSe nanoparticles was the current range of 20−120mA/cm^2. We also found that the reaction time almost did not affect the particle size. For reaction times of 10, 30, or 60 min, the same particle size of 12 nm was obtained. We have measured the particle size for a constant amount of electricity while changing other parameters. In the two experiments where the total amount of electricity is the same, the current and elapsed time are changed. The conditions were $t = 30$ min, $I = 50$ mA and $t = 15$ min, $I = 100$ mA. For both cases the current efficiency was approximately the same (72%). The measured particle size for the lower current was 12 nm, while for the high current, a 10 nm size is obtained. We conclude that Winand's claim that the higher the current density or overpotential the smaller are the nuclei and the faster is the nucleation is correct.[46−47]

In general, decreasing temperature, shorter pulse duration and higher sonic intensity, and lower current density all lead to a decrease of the PbSe particle size.

Conclusions

PbSe nanoparticles have been prepared by the sono-electrochemical method whereby the nanoparticle sizes were controlled over a 10−16-nm range, using different deposition parameters. The advantages of this process are that it is a simple and efficient method for producing nanoparticles. We can foresee the upscaling of the process to form large quantities of nanosized PbSe. These nanoparticles could find use in photoresistors, photodetectors, and photoemitters.

Acknowledgment. Dr. Zhu thanks the Kort 100 Scholarship Foundation for supporting his postdoctoral fellowships. Dr. Zhu also grateful for the support of the China Scholarship Council. Dr. Yuri Koltypin thanks the Ministry of Absorption, The Center for Absorption in Sciences, for its financial support. Professor A. Gedanken thanks the German Ministry of Science through the Deutche-Israeli program DIP for its support and gratefully acknowledges receipt of a NEDO International Joint Research Grant. The authors are grateful to Professor M. Deutsch, Department of Physics, Professor Z. Malik, Department of Life Sciences, and Dr. A. Zaban, Department of Chemistry, for extending their facilities to us. Kind assistance from Dr. Jeevanandam is gratefully acknowledged. We also thank Dr. Shifra Hochberg for editorial assistance.

CM990459W

(46) Winand, R. *Hydrometallurgy* **1992**, *29*, 567.
(47) Winand, R. *Application of Polarization Measurements in the Control of Metal Deposition*; Warren, I. H., Ed., Elsevier: Amsterdam, 1984.